Spin squeezing of a dipolar Bose gas in a double-well potential

Qing-Shou Tan,[1,2] Hai-Yan Lu,[3] and Su Yi[2,*]

[1]*College of Physics and Electronic Engineering, Hainan Normal University, Haikou 571158, China*

[2]*State Key Laboratory of Theoretical Physics, Institute of Theoretical Physics, Chinese Academy of Sciences, P. O. Box 2735, Beijing 100190, China*

[3]*Science and Technology on Surface Physics and Chemistry Laboratory, Mianyang 621908, Sichuan, China*

(Received 2 November 2015; published 11 January 2016)

The spin-squeezing dynamics of a quasi-one-dimensional dipolar Bose gas trapped in a double-well potential is studied by employing the method of the multiconfigurational time-dependent Hartree for bosons. We find that optimal squeezing generated by the dipolar interaction can be improved over the one-axis twisting limit, and this squeezing is much stronger than that obtained by the contact interaction. Moreover, natural orbital-related squeezing can be controlled by the direction of the dipole moment, which provides control for storing the optimal spin squeezing. The origin of the squeezing as well as the relationship between spin squeezing and the two-order correlation function are also discussed.

DOI: 10.1103/PhysRevA.93.013606

I. INTRODUCTION

Bose-Einstein condensates (BECs) trapped in an external double-well potential have attracted much attention due to their potential applications in quantum information and quantum metrology [1–7]. This two-component BEC with the one-axis twisting (OAT) interaction is a useful resource for preparing spin-squeezed state [9–18]. Spin squeezing (SS) arising from quantum correlation is widely used to study many-body correlations and entanglement, as well as to improve the precision of measurements [14]. The use of spin-squeezing parameters as many-body entanglement witnesses has already been discussed in Ref. [15]. Additionally, Kitagawa *et al.* [9] and Wineland *et al.* [10] proposed using atomic squeezed states in order to reduce quantum noise in interferometry to beat the standard quantum limit.

Due to these applications, squeezed states in a double-well BEC have been widely studied, both experimentally [7,8] and theoretically [19–21]. However, in almost all the theoretical works, bosons are assumed to reside in several fixed orbitals, which captures the basic processes and physics but ignores entirely the spatial evolution of the condensate wave functions. It is well known that for weakly interacting gases, the famous time-dependent Gross-Pitaevskii equation (GPE) is a good description of the spatial evolution of the condensate [18,22,23]. However, the mean-field theory cannot describe the atom number fluctuation of the condensate well. Thus, we cannot directly obtain the SS parameter by using the GPE. Therefore, Cederbaum *et al.* developed the multiconfigurational time-dependent Hartree for bosons method (MCTDHB) [24,25], which allows us to describe both the atom number and the spatial dynamics in a self-consistent fashion. The MCTDHB(M) method describes the dynamics of the many-body wave function by assuming that the bosons can only occupy M orthonormal orbitals. Recently, according to the MCTDHB theory, Grond *et al.* [4–6] successfully developed and implemented an optimal quantum control approach for BECs in a double-well potential. They simulated the splitting dynamics process [4,5] and they designed controls for fast Mach-Zehnder interferometry operations [6] to obtain the high parameter-estimation precision.

Up to now, studies of bosonic atoms trapped in a double-well potential have focused mainly on s-wave contact interaction. For ultracold, there also exists long-range dipole-dipole interaction (DDI), which may have a significant effect on the stability of the condensate [26] and generate a variety of novel quantum phases [27–30] as well as translational entanglement [31]. Furthermore, both the sign and the strength of the effective dipolar interaction can be tuned via a fast rotating orienting field [32–34]. A controllable interatomic interaction beyond short-range isotropic character would greatly enrich the available toolbox for quantum information and quantum metrology. However, the powerful MCTDHB theory, including the DDI, was seldom used in studying the SS dynamics of bosonic atoms trapped in a double-well potential.

In this paper, we apply the MCTDHB(2) to consider the spatial dynamics in order to obtain a realistic description of the SS dynamics induced by the two-body interaction. In contrast with the usually considered two-mode model in double-well BECs, here we eliminate the concept of left and right orbitals. In addition, we demonstrate that the SS dynamics between the atoms resided in the natural orbitals for the system initially prepared in a coherent state. Essentially, this squeezing is the macroscopic quantum correlation between the ground and first excited states in the condensates. We show that compared with the contact interaction, the dipolar interaction can generate better squeezing. In addition, the optimal values of this squeezing can be improved over the OAT limit. Moreover, this enhanced squeezing can be controlled by tuning the direction of the dipole moment, which realizes the storage of the optimal squeezing. The significant advantage of the DDI is this enhanced and controllable squeezing.

The paper is organized as follows. In Sec. II, we give the model of atoms trapped in a quasi-one-dimensional (1D) double-well potential, and we briefly review the MCTDHB theory as well as the spin-squeezing parameter. In Sec. III, we investigate the SS dynamics due to the two-body interaction,

*syi@itp.ac.cn

and we compare the optimal squeezing generated by contact interaction with the dipolar interaction. Finally, we discuss the origin of the squeezing as well as the relationship between the SS and the two-order correlation function.

II. FORMULATION

A. Model

We consider a system of N polarized (along the direction $\hat{\mathbf{d}}$) bosonic dipoles trapped in a quasi-1D double-well potential. In second-quantized form, the many-body Hamiltonian is

$$\hat{H} = \int dx \hat{\Psi}^\dagger(x)\hat{h}\hat{\Psi}(x) + \frac{1}{2}\int dx\, dx' \hat{\Psi}^\dagger(x)\hat{\Psi}^\dagger(x')V(x-x')\hat{\Psi}(x')\hat{\Psi}(x), \quad (1)$$

where $\hat{\Psi}(x)$ is the field operator and $\hat{h} = -\frac{\hbar^2\partial^2}{2m\partial x^2} + U(x)$ is the single-particle Hamiltonian, with m being the mass of the atom and $U(x)$ being the trap. More specifically, we assume that the trapping potential is a symmetric double well, i.e.,

$$U(x) = \tfrac{1}{2}m\omega^2x^2 + U_0e^{-x^2/(2\sigma^2)}, \quad (2)$$

where ω is the trap frequency, and U_0 and σ are, respectively, the height and width of the barrier. In three dimensions, the two-body interaction is

$$V^{(3D)}(\mathbf{r}) = c_0\delta(\mathbf{r}) + c_d\frac{1-3(\hat{\mathbf{d}}\cdot\hat{\mathbf{r}})^2}{r^3}, \quad (3)$$

where the contact interaction strength is $c_0 = 4\pi\hbar^2a_0/m$, with a_0 being the s-wave scattering length; the dipolar interaction strength is $c_d = \mu_0d^2/(4\pi)$, with μ_0 being the vacuum permeability and d the magnetic dipole moment; and $\hat{\mathbf{r}} = \mathbf{r}/r$ is a unit vector.

To obtain the effective 1D interaction potential, $V(x-x')$, in Hamiltonian (1), we assume that the transverse wave function of all atoms is

$$\phi_\perp(y,z) = \frac{1}{q\sqrt{\pi}}e^{-(y^2+z^2)/(2q^2)}, \quad (4)$$

with q being the width of the Gaussian function. Without loss of generality, we assume that the dipole moments lie on the xz plane forming an angle α to the z axis, i.e.,

$$\hat{\mathbf{d}} = (\sin\alpha, 0, \cos\alpha). \quad (5)$$

The effective 1D interaction potential can then be obtained by integrating out the y and z variables as

$$\begin{aligned} V(x-x') &= \int dy\, dz\, dy'dz' |\phi_\perp(y,z)|^2 V^{(3D)}(\mathbf{r}-\mathbf{r}')|\phi_\perp(y',z')|^2 \\ &= \frac{c_0}{2\pi q^2}\delta(x-x') + \frac{\chi_\alpha c_d}{q^5}\left[q|x-x'| - \sqrt{\frac{\pi}{2}}(q^2+|x-x'|^2)e^{|x-x'|^2/(2q^2)}\mathrm{erfc}\left(\frac{|x-x'|}{\sqrt{2}q}\right)\right], \end{aligned} \quad (6)$$

where $\mathrm{erfc}(\cdot)$ is the complementary error function and

$$\chi_\alpha = 1 - \tfrac{3}{2}\sin^2\alpha \quad (7)$$

is an angle-dependent coefficient that makes the dipolar interaction strength tunable. Clearly, the effective 1D dipolar interaction vanishes at the magical angle $\alpha_m \simeq 54.7^\circ$, and it is repulsive (attractive) for $\alpha < \alpha_m$ ($\alpha > \alpha_m$). Finally, we point out that the contact interaction strength c_0 is also tunable via Feshbach resonance.

B. MCTDHB

To proceed, let us briefly outline the MCTDHB(2) approach. We assume that atoms can only reside in two orbitals, $\{\psi_\mu(x,t)\}_{\mu=1,2}$, which satisfy the orthonormal conditions $\int dx\, \psi_\mu^*(x,t)\psi_\nu(x,t) = \delta_{\mu\nu}$. The field operator in Hamiltonian (1) can then be expanded as $\hat{\Psi}(x) = \sum_{\mu=1,2} b_\mu(t)\psi_\mu(x,t)$, where $b_\mu(t) = \int dr\, \psi_\mu^*(r,t)\hat{\Psi}(r)$ are the bosonic annihilation operators. With this two-orbital assumption, the Hamiltonian (1) can be written as

$$\hat{H} = \sum_\mu h_{\mu\mu}b_\mu^\dagger b_\mu + \frac{1}{2}\sum_{\mu,\mu',\nu,\nu'} V_{\mu\mu'\nu\nu'}b_\mu^\dagger b_{\mu'}^\dagger b_\nu b_{\nu'}, \quad (8)$$

where $h_{\mu\mu} = \int dx\, \psi_\mu^*(x)\hat{h}\psi_\mu(x)$, and

$$V_{\mu\mu'\nu\nu'} = \int dx\, dx' \psi_\mu^*(x)\psi_{\mu'}^*(x')V(x-x')\psi_{\nu'}(x')\psi_\nu(x) \quad (9)$$

is the interaction matrix elements.

Now, the wave function of the system takes the general form

$$|\Psi(t)\rangle = \sum_n C_n(t)|n,t\rangle, \quad (10)$$

where C_n are the expansion coefficients and

$$|n\rangle \equiv |n, N-n\rangle = \frac{1}{\sqrt{n!(N-n)!}}(b_1^\dagger)^n(b_2^\dagger)^{N-n}|\mathrm{vac}\rangle \quad (11)$$

are the basis states that preserve the total number of particles.

According to the MCTDHB theory, the expansion coefficients $\{C_n\}$ and the orbitals $\{\psi_\alpha\}$ are determined self-consistently through the variational principle [24,25]. Using the Lagrangian formulation, it is found that the expansion coefficients satisfy the equations

$$i\hbar\frac{\partial C_n}{\partial t} = \sum_{n'}\langle n|\hat{H}|n'\rangle C_{n'}. \quad (12)$$

The dynamic equations governing the orbitals are [24,25,30]

$$\begin{aligned} i\hbar\frac{\partial\psi_1}{\partial t} &= \left[\hat{h} + \gamma_{11}^{-1}W_{11}(x) + \gamma_{12}^{-1}W_{21}(x) - p_{11}\right]\psi_1 \\ &\quad + \left[\gamma_{11}^{-1}W_{12}(r) + \gamma_{12}^{-1}W_{22}(x) - p_{12}\right]\psi_2, \end{aligned} \quad (13)$$

$$\begin{aligned} i\hbar\frac{\partial\psi_2}{\partial t} &= \left[\hat{h} + \gamma_{21}^{-1}W_{12}(x) + \gamma_{22}^{-1}W_{22}(x) - p_{22}\right]\psi_2 \\ &\quad + \left[\gamma_{21}^{-1}W_{11}(x) + \gamma_{22}^{-1}W_{21}(x) - p_{21}\right]\psi_1, \end{aligned} \quad (14)$$

where

$$\gamma_{\alpha\beta} = \langle\Psi|\hat{b}_\alpha^\dagger \hat{b}_\beta|\Psi\rangle \tag{15}$$

is the one-body density matrix, with γ^{-1} being the inverse of γ,

$$W_{\alpha\beta}(x) = \sum_{\alpha'\beta'} \Gamma_{\alpha\alpha'\beta\beta'} \int dx' \psi_{\alpha'}^*(x') V(x-x') \psi_{\beta'}(x'), \tag{16}$$

with

$$\Gamma_{\alpha\alpha'\beta\beta'} = \langle\Psi|\hat{b}_\alpha^\dagger \hat{b}_{\alpha'}^\dagger \hat{b}_\beta \hat{b}_{\beta'}|\Psi\rangle \tag{17}$$

being the two-body density matrix, and

$$p_{\sigma\zeta} = h_{\sigma\zeta} + \sum_{\alpha,\beta} \gamma_{\sigma\alpha}^{-1} \int dx' \psi_\zeta^*(x') W_{\alpha\beta}(x-x') \psi_\beta(x). \tag{18}$$

Then, the dynamical behavior of the system is completely determined by the coupled Eqs. (12)–(14).

C. Spin-squeezing parameter

Similar to the two-mode system with fixed mode functions, we define the pseudo-spin-operator $\mathbf{J} \equiv (J_x, J_y, J_z)$ based on the time-dependent natural orbitals as $\hat{J}_i = \frac{1}{2}\sum_{\alpha\beta} \hat{b}_\alpha^\dagger \sigma_{\alpha\beta}^{(i)} \hat{b}_\beta$, where $\sigma^{(i)}$ are the Pauli matrices. Now, a state is regarded as squeezed if the variance of one spin component normal to the mean spin vector $\langle \boldsymbol{J}\rangle = \langle\Psi(t)|\boldsymbol{J}|\Psi(t)\rangle$ is lower than the Heisenberg limited value. Mathematically, the SS parameter is [9]

$$\xi^2 = \frac{4(\Delta J_{\hat{n}_\perp})_{\min}^2}{N}, \tag{19}$$

where $(\Delta J_{\hat{n}_\perp})_{\min}$ represents the minimal variance of the spin component perpendicular to the mean spin direction $\hat{n}_0 \equiv \langle\mathbf{J}\rangle/|\langle\mathbf{J}\rangle|$. A state is spin-squeezed and entangled if $\xi^2 < 1$. In addition, the smaller ξ^2 is, the stronger is the squeezing.

The squeezing parameter Eq. (19) can be evaluated explicitly [14]. Toward that end, we assume, without loss of generality, that $\hat{n}_0 = (\sin\vartheta\cos\varphi, \sin\vartheta\sin\varphi, \cos\vartheta)$, where $\vartheta = \tan^{-1}(\sqrt{\langle J_x\rangle^2 + \langle J_y\rangle^2}/\langle J_z\rangle)$ and $\varphi = \tan^{-1}(\langle J_y\rangle/\langle J_x\rangle)$ are polar and azimuthal angles, respectively. We then define two mutually perpendicular unit vectors $\hat{n}_1 = (-\sin\varphi, \cos\varphi, 0)$ and $\hat{n}_2 = (\cos\vartheta\cos\varphi, \cos\vartheta\sin\varphi, -\sin\vartheta)$. Clearly, both $\hat{n}_1$ and $\hat{n}_2$ are perpendicular to $\hat{n}_0$ such that $(\hat{n}_1, \hat{n}_2, \hat{n}_0)$ form a right-hand frame. Now, the squeezing parameter can be expressed as [14]

$$\xi^2 = \frac{2}{N}\left[\langle J_{\hat{n}_1}^2 + J_{\hat{n}_2}^2\rangle - \sqrt{\left(\langle J_{\hat{n}_1}^2 - J_{\hat{n}_2}^2\rangle\right)^2 + \left(\langle[J_{\hat{n}_1}, J_{\hat{n}_2}]_+\rangle\right)^2}\right], \tag{20}$$

where $[A,B]_+ = AB + BA$ represents the anticommutator. Moreover, for our model, it can be shown that

$$\begin{aligned}\langle J_{\hat{n}_1}^2\rangle &= -\tfrac{1}{2}\left[\Gamma_{1122}^{(r)}\cos(2\varphi) + \Gamma_{1122}^{(i)}\sin(2\varphi)\right] \\ &\quad + \tfrac{1}{4}(2\Gamma_{1212} + \gamma_{11} + \gamma_{22}),\end{aligned} \tag{21}$$

$$\begin{aligned}\langle J_{\hat{n}_2}^2\rangle &= \tfrac{1}{4}\left(2\Gamma_{1122}^{(r)} + 2\Gamma_{1212} + \gamma_{11} + \gamma_{22}\right)\sin^2\vartheta\cos^2\varphi \\ &\quad - \tfrac{1}{4}\left(2\Gamma_{1122}^{(r)} - 2\Gamma_{1212} - \gamma_{11} - \gamma_{22}\right)\cos^2\vartheta\sin^2\varphi \\ &\quad + \tfrac{1}{4}\left(\Gamma_{1111} + \Gamma_{2222} - 2\Gamma_{1212} + \gamma_{11} + \gamma_{22}\right)\sin^2\vartheta \\ &\quad - \tfrac{1}{2}\left[\Gamma_{1112}^{(r)} + \Gamma_{1112}^{(i)} - \Gamma_{1222}^{(r)} - \Gamma_{1222}^{(i)}\right]\sin(2\vartheta)\cos\varphi \\ &\quad + \tfrac{1}{2}\Gamma_{1122}^{(i)}\cos^2\vartheta\sin(2\varphi)\end{aligned} \tag{22}$$

and

$$\begin{aligned}\left\langle\left[J_{\hat{n}_1}, J_{\hat{n}_2}\right]_+\right\rangle &= -\Gamma_{1122}^{(r)}\sin(2\varphi)\cos\vartheta + \Gamma_{1122}^{(i)}\cos(2\varphi)\cos\vartheta \\ &\quad + \left(\Gamma_{1112}^{(r)} - \Gamma_{1222}^{(r)}\right)\sin\varphi\sin\vartheta \\ &\quad - \left(\Gamma_{1112}^{(i)} - \Gamma_{1222}^{(i)}\right)\cos\varphi\sin\vartheta,\end{aligned} \tag{23}$$

where $\Gamma_{\alpha\alpha'\beta\beta'}^{(r)}$ and $\Gamma_{\alpha\alpha'\beta\beta'}^{(i)}$ represent, respectively, the real and imaginary parts of $\Gamma_{\alpha\alpha'\beta\beta'}$.

III. SPIN SQUEEZING GENERATED BY THE DIPOLE-DIPOLE INTERACTION

In this section, we study the dynamical generation of SS in dipolar condensates trapped in a double-well potential. As a concrete example, we consider a BEC of ^{162}Dy atoms, for which we have $d = 9.9\mu_B$ and $a_0 = 112a_B$, with μ_B and a_B the Bohr magneton and Bohr radius, respectively [35]. Numerically, it is convenient to introduce the following dimensionless units: $\hbar\omega$ for energy, ω^{-1} for time, and $\ell = [\hbar/(m\omega)]^{1/2}$ for length. To reduce the number of free parameters, we assume that $\omega = (2\pi)10$ Hz, $q/\ell = 0.1$, and $\sigma/\ell = 2$ throughout the paper. Consequently, the system is completely characterized by the following parameters: the particle number N, the scattering length a_0, the dipole moment of atoms d, and the direction of the dipole moment α.

To see how the SS is generated by the interactions, the initial state is prepared as the ground state of the double-well potential with $U_0 = 15\hbar\omega$ in the absence of any interactions. Namely, at $t = 0$ all the atoms condense into the symmetric orbital ψ_1 [see Fig. 1(a)], and the expansion coefficient C_N is unit.

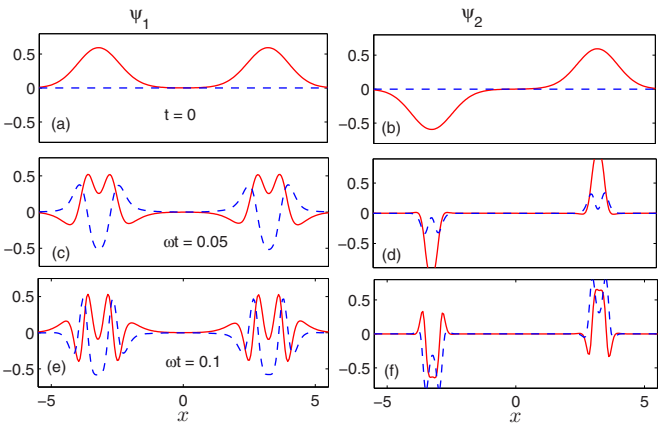

FIG. 1. Natural orbitals ψ_1 and ψ_2 at $\omega t = 0$, 0.05, and 0.1 after the contact interaction is turned on at $t = 0$. The red solid lines and the blue dashed lines are, respectively, the real and imaginary parts of ψ_1 and ψ_2. Other parameters are $N = 500$, $\alpha = 0^\circ$, and $U_0 = 20\hbar\omega$.

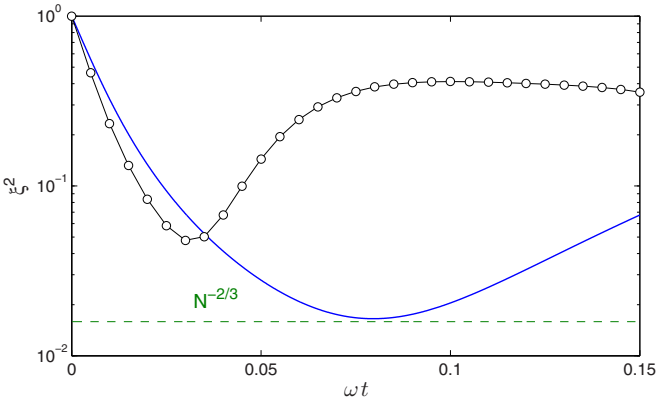

FIG. 2. Comparison of dynamical behaviors of the SS parameter ξ^2 obtained with fixed orbits (blue solid line) and the MCTDHB(2) method (black empty circles). Here $N = 500$, $\alpha = 0^\circ$, and $U_0 = 20\hbar\omega$.

A. Spin squeezing generated by the contact interaction

First we briefly review the SS dynamics of the generic two-mode model, in which the time evolutions of the mode functions are ignored. For initial symmetry and antisymmetry orbitals [see Figs. 1(a) and 1(b)], we have $V_{1111} = V_{2222} = V_{1122} = V_{1212} = V_{1221} = \kappa$ and $V_{1112} = V_{2221} = 0$. Therefore, Hamiltonian (8) is reduced to $H = \delta_0 J_z + 2\kappa J_x^2$ with $\delta_0 = h_{11} - h_{22}$ [2]. This corresponds to the widely studied OAT interaction, for which the optimal squeezing value for this mode is $\sim N^{-2/3}$. However, in fact, as shown in Fig. 1, with time increasing the orbitals have spatial evolution and can also acquire additional phases. Therefore, assuming *a priori* fixed orbitals is not a realistic description of the condensates. So we should reexamine the SS induced by contact interaction in a double-well potential with the MCTDHB method.

In Fig. 2, we compare the dynamical behaviors of the squeezing parameter ξ^2 obtained by the generic two-mode model with the MCTDHB(2) theory. As is shown, the dynamical behaviors of ξ^2 obtained by these two methods do not coincide with each other, either in the optimal squeezing value or at the maximal-squeezing time. When performing the MCTDHB(2), the value of the optimal squeezing is not able to reach the OAT limit $\sim N^{-2/3}$ as that obtained from the generic two-mode model because of the spatial evolution of the condensate wave functions.

Therefore, the widely studied OAT mode, which is derived from fixed spatial wave functions, cannot exactly describe the SS behaviors of the Bose gas trapped in a double-well potential. In addition, the OAT squeezing limit cannot be obtained by the contact interaction. To obtain high SS, we should consider the long-range interaction.

B. Spin squeezing generated by the dipolar interaction

We now investigate the SS generated by the long-range dipolar interaction and compare it with the contact interaction using the MCTDHB(2) method. To give a visual comparison, we first illustrate the squeezing process by calculating the Husimi Q function [14],

$$Q(\theta,\phi) = |\langle\theta,\phi|\Psi(t)\rangle|^2, \tag{24}$$

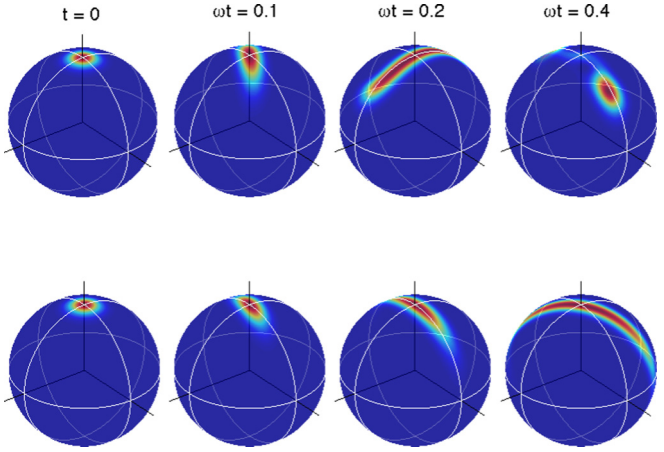

FIG. 3. Husimi Q function of spin-squeezed states generated by contact interaction (the top panel) and dipolar interaction (the bottom panel) for various times: $\omega t = 0$, 0.1, 0.2, and 0.4. At the beginning, $t = 0$, the state is a CSS and thus the Q function is a circle. The optimal squeezing angle rotates around the z axis with time. Here $\alpha = 0^\circ$, $N = 100$, and $U_0 = 20\hbar\omega$.

which represents the quasiprobability distribution of $\Psi(t)$, and $|\theta,\phi\rangle$ is the coherent spin state (CSS), with θ and ϕ the polar and azimuthal angles. In Fig. 3, we show the Husimi Q function of spin-squeezed states generated by the two-body interaction on the Bloch sphere. The top and bottom panels, respectively, correspond to the SS generated by the contact and the dipolar interaction. As we can see, at $t = 0$ the initial CSS is a circle given by the Husimi function, and, during the evolution, the Husimi Q function becomes squeezed and elliptical while the squeezing angle rotates. Comparing the two panels in Fig. 3, we can see that the distribution corresponding to the DDI is more elongated and narrower than that of the contact interaction. This indicates that the long-range DDI can generate better squeezing.

The dynamical evolution of the SS parameter ξ^2 for different angle α is plotted in Fig. 4(a). It is shown that the optimal squeezing generated by the dipolar interaction can be improved over the OAT limit, which scales as $\sim N^{-2/3}$. In addition, the optimal squeezing points change with α. When α approaches the magical angle α_m, the maximal-squeezing time t^* becomes larger and larger. As considered in [32,33], if $\alpha = \alpha_m \simeq 54.7^\circ$, the dipolar interaction averages to zero, and then at this angle there is no dipolar interaction to induce SS. This means that the angle-dependent squeezing provides the possibility to store the optimal squeezing by making $\alpha = \alpha_m$ at maximal-squeezing time t^*. Therefore, the enhanced and controllable squeezing induced by DDI has significant advantages when compared with that induced by contact interaction.

To check if the advantages of DDI remain valid for large atom numbers N, we study the SS quantities with respect to N in Fig. 4(b). It is clear that with the increase in the atom number N, the optimal SS generated by the DDI will tend to a steady value, which is worse than the OAT limit. However, the optimal squeezing values are still better than that generated by the contact interaction.

Next, we shall investigate the origin of the sub-shot-noise limit SS. We first decompose the interaction Hamiltonian

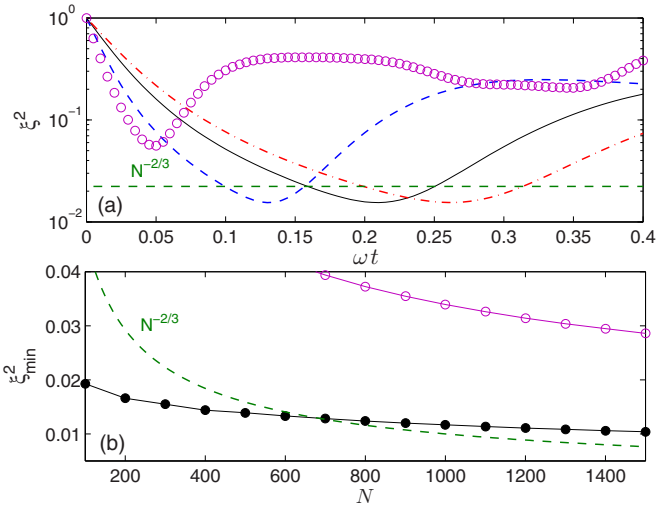

FIG. 4. (a) Dynamical evolution of the spin-squeezing parameter ξ^2 for different angle α: $\alpha = 0^\circ$ (blue dashed curve), $\alpha = 30^\circ$ (black solid curve), and $\alpha = 90^\circ$ (red dashed-dotted curve). Compared with the contact interaction (empty circles), the squeezing for the dipolar interaction is much stronger. Here $N = 300$ and $U_0 = 20\hbar\omega$. (b) Optimal squeezing parameter as a function of atom number N, where the black solid circles and the empty circles, respectively, present the SS generated by the DDI and the contact interaction.

(8) into

$$H = H_1 + H_2 + H_3, \tag{25}$$

$$H_1 = \delta J_z + \chi J_z^2, \tag{26}$$

$$H_2 = \tfrac{1}{2}(\beta J_+ + \beta^* J_-), \tag{27}$$

$$H_3 = \tfrac{1}{2}(V_{1122} J_+^2 + V_{1122}^* J_-^2). \tag{28}$$

Here H_1 is the generalized OAT Hamiltonian with $\delta = h_{11} - h_{22} + (V_{1111} - V_{2222})(\hat{N} - 1)/2$ and $\chi = [V_{1111} + V_{2222} - 2(V_{1212} + V_{1221})]/2$. This type of Hamiltonian has been widely used to generate squeezing for the two-mode model, however for our initial state (all atoms condensed into the first orbital ψ_1) it will not contribute squeezing for a short time. In addition, H_2 describes one-particle exchanges between the orbitals, where $\beta = (V_{1112} + V_{1222})\hat{N} + (V_{1112} - V_{1222})J_z$ with $\hat{N} = b_1^\dagger b_1 + b_2^\dagger b_2$. The dynamic behaviors of V_{1122} and V_{1222} for DDI and contact interaction are, respectively, displayed in Figs. 5(c) and 5(d). As is shown in Fig. 6, the Hamiltonian H_2 also cannot directly induce squeezing for our initial state.

Therefore, the squeezing is mainly due to H_3, which is analogous to the two-axis twisting Hamiltonian [9] for exchanging two particles between the two natural orbitals. It is well known that the two-axis twisting scheme can provide stronger squeezing than OAT. This can be used to explain the enhanced squeezing illustrated in Fig. 4.

To demonstrate the effects of H_3 on squeezing for both the long-range DDI and short-range contact interaction, we compare in Figs. 5(a) and 5(b) the values of the two-particle exchange parameter V_{1122} for dipolar and contact interaction with respect to time ωt. These figures show that both the

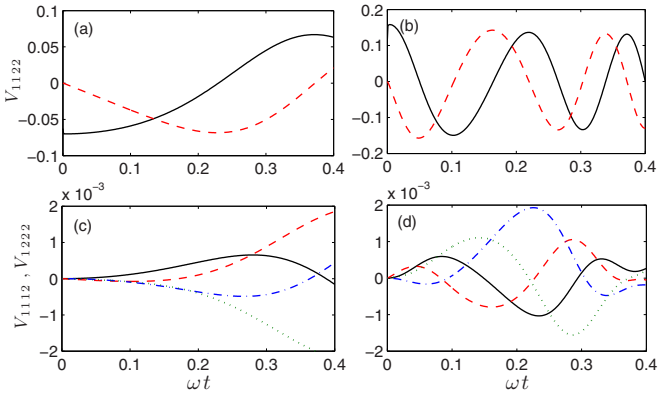

FIG. 5. Parts (a) and (b), respectively, plot the two-particle exchange parameter V_{1122} for dipolar and contact interaction as a function of ωt. Parts (c) and (d), respectively, show the parameters V_{1112} and V_{1222} for dipolar and contact interaction as a function of ωt. In (a) and (b), the black solid (red dashed) curves represent the real (imaginary) parts of V_{1122}. In (c) and (d), the black solid (red dashed) curves represent the real (imaginary) parts of V_{1122}, and the blue dot-dashed (green dotted) curves represent the real (imaginary) parts of V_{1222}. Other parameters are $\alpha = 0^\circ$, $N = 300$, and $U_0 = 20\hbar\omega$.

real and imaginary parts of V_{1122} oscillate with time. During the time scale of maximal-squeezing time t^*, the value of V_{1122} for dipolar interaction gradually changes. However, the case for contact interaction [see Fig. 5(b)] illustrates periodic oscillation, which results in the SS, $\xi^2_{H_3}$, generated by H_3 being worse than that obtained by DDI. In Fig. 6(b), we can see that for DDI the optimal squeezing value of $\xi^2_{H_3}$ is improved over the OAT limit. Figure 6 also shows that the squeezing values of both the contact interaction and DDI are mainly from Hamiltonian H_3, especially for a short time. However, as the time increases, H_1 and H_2 will modify the optimal squeezing values and maximal-squeezing time. For DDI, the effect of H_1 and H_2 will slightly increase the squeezing generated by H_3, but the case is completely different for contact interaction.

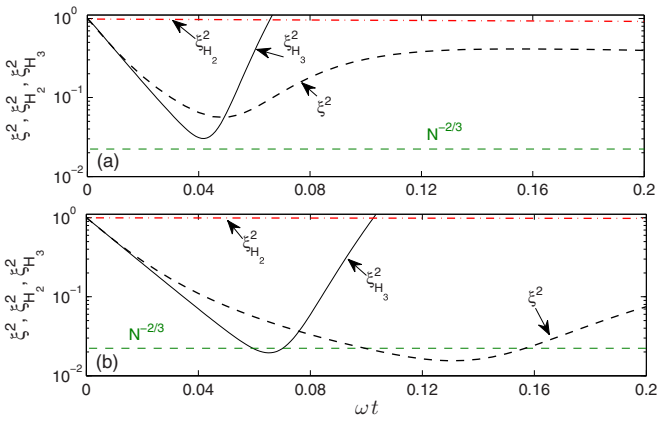

FIG. 6. Dynamical behaviors of the SS parameter obtained by the Hamiltonian H_2, the Hamiltonian H_3, and the total Hamiltonian H. Parts (a) and (b), respectively, correspond to the SS generated by the contact interaction and DDI. Here $N = 300$, $\alpha = 0^\circ$, and $U_0 = 20\hbar\omega$.

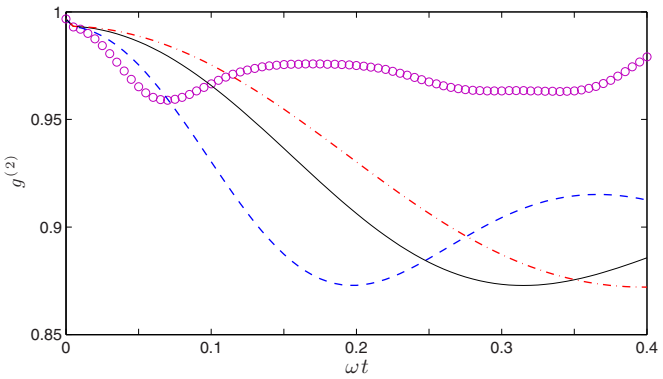

FIG. 7. The second-order correlation function $g^{(2)}$ vs time ωt for different angles. Parameters are the same as for Fig. 4(a).

C. Spin-squeezing and second-order correlation function

Notice that, in general, the squeezing obtained by the MCTDHB approach has no direct correspondence with that obtained by the usual two-mode model. This is because MCTDHB, which relies on time-dependent orbitals, may also capture a large class of excitations not included in a two-mode model [5]. Therefore, it may be difficult to detect the squeezing exactly through the widely used time-of-flight measurement. However, there is a close relationship between the SS and the second-order correlation function in our model.

Now we consider the second-order correlations between the two atomic modes [36],

$$g^{(2)} \equiv \frac{\langle b_1^\dagger b_1 b_2^\dagger b_2\rangle}{\langle b_1^\dagger b_1\rangle\langle b_2^\dagger b_2\rangle} = \frac{\Gamma_{1212}}{\gamma_{11}\gamma_{22}}, \tag{29}$$

which describe the probability of detecting a particle in the first excited state ψ_2 with a given particle in the ground state ψ_1.

In Fig. 7, we plot the second-order correlation function $g^{(2)}$ as a function of time ωt. Compared with Fig. 4(a), we can find that $g^{(2)}$ and ξ^2 have almost the same changing trend, except that the minimal values of $g^{(2)}$ have a little time delay. This gives us a way to detect the SS indirectly.

IV. CONCLUSION

In summary, we have investigated the dynamical generation of SS between the atoms in two natural orbitals by using the MCTDHB(2) method. Compared with the usual two-mode model, which ignores entirely the spatial evolution of the condensate wave functions, the calculation based on the MCTDHB is more reliable. We have shown that the squeezing generated by the dipolar interaction can be better than the OAT limit, and also much stronger than that obtained by the contact interaction. In particular, we found that the enhanced squeezing can be stored by adjusting the direction of the dipole moment. To explain the enhanced squeezing, we investigated the origin of the squeezing. It is found that enhanced squeezing is mainly due to the two-particle exchanging interaction, which is analogous to the two-axis twisting scheme and has advantages for generating SS. Finally, we demonstrated the close relationship between the squeezing and the second-order correlation function, which may provide an indirect way to detect the squeezing.

ACKNOWLEDGMENTS

This work was supported by the National 973 program (Grant No. 2012CB922104) and the NSFC (Grants No. 11434011, No. 11421063, No. 11547159, No. 11375059, and No. 11565011). H.-Y. L. acknowledges support from the NSFC under Grant No. 11404299.

[1] G. J. Milburn, J. Corney, E. M. Wright, and D. F. Walls, Phys. Rev. A **55**, 4318 (1997).
[2] J. Javanainen and M. Y. Ivanov, Phys. Rev. A **60**, 2351 (1999).
[3] L. Pezzé, L. A. Collins, A. Smerzi, G. P. Berman, and A. R. Bishop, Phys. Rev. A **72**, 043612 (2005).
[4] J. Grond, J. Schmiedmayer, and U. Hohenester, Phys. Rev. A **79**, 021603 (2009).
[5] J. Grond, U. Hohenester, I. Mazets, and J. Schmiedmayer, New J. Phys. **12**, 065036 (2010).
[6] J. Grond, G. von Winckel, J. Schmiedmayer, and U. Hohenester, Phys. Rev. A **80**, 053625 (2009).
[7] J. Estève, C. Gross, A. Weller, S. Giovanazzi, and M. K. Oberthaler, Nature (London) **455**, 1216 (2008).
[8] T. Berrada, S. van Frank, R. Bücker, T. Schumm, J. F. Schaff, and J. Schmiedmayer, Nat. Commun. **4**, 2077 (2013).
[9] M. Kitagawa and M. Ueda, Phys. Rev. A **47**, 5138 (1993).
[10] D. J. Wineland, J. J. Bollinger, W. M. Itano, and D. J. Heinzen, Phys. Rev. A **50**, 67 (1994).
[11] A. Sørensen, L.-M. Duan, J. I. Cirac, and P. Zoller, Nature (London) **409**, 4 (2001).
[12] U. V. Poulsen and K. Mølmer, Phys. Rev. A **64**, 013616 (2001).
[13] G. R. Jin, Y. C. Liu, and W. M. Liu, New J. Phys. **11**, 073049 (2009).
[14] J. Ma, X. Wang, C. P. Sun, and F. Nori, Phys. Rep. **509**, 89 (2011).
[15] O. Guehne and G. Tóth, Phys. Rep. **474**, 1 (2009).
[16] X. Wang and B. C. Sanders, Phys. Rev. A **68**, 012101 (2003).
[17] Y. C. Liu, Z. F. Xu, G. R. Jin, and L. You, Phys. Rev. Lett. **107**, 013601 (2011).
[18] S. A. Haine, J. Lau, R. P. Anderson, and M. T. Johnsson, Phys. Rev. A **90**, 023613 (2014).
[19] G. R. Jin, Y. An, T. Yan, and Z. S. Lu, Phys. Rev. A **82**, 063622 (2010).
[20] B. Juliá-Díaz, T. Zibold, M. K. Oberthaler, M. Melé-Messeguer, J. Martorell, and A. Polls, Phys. Rev. A **86**, 023615 (2012).
[21] C. Gross, J. Phys. B **45**, 103001 (2012).
[22] D. Ananikian and T. Bergeman, Phys. Rev. A **73**, 013604 (2006).

[23] H.-Y. Lu, H. Lu, J.-N. Zhang, R.-Z. Qiu, H. Pu, and S. Yi, Phys. Rev. A **82**, 023622 (2010).
[24] A. I. Streltsov, O. E. Alon, and L. S. Cederbaum, Phys. Rev. A **73**, 063626 (2006).
[25] O. E. Alon, A. I. Streltsov, and L. S. Cederbaum, Phys. Rev. A **77**, 033613 (2008).
[26] S. Yi and L. You, Phys. Rev. A **61**, 041604(R) (2000); **63**, 053607 (2001).
[27] K. Goral, L. Santos, and M. Lewenstein, Phys. Rev. Lett. **88**, 170406 (2002).
[28] S. Yi, L. You, and H. Pu, Phys. Rev. Lett. **93**, 040403 (2004).
[29] S. Yi, T. Li, and C. P. Sun, Phys. Rev. Lett. **98**, 260405 (2007).
[30] H.-Y. Lu and S. Yi, Sci. China-Phys. Mech. Astron. **55**, 1535 (2012).
[31] T. Opatrný, B. Deb, and G. Kurizki, Phys. Rev. Lett. **90**, 250404 (2003).
[32] S. Giovanazzi, A. Görlitz, and T. Pfau, Phys. Rev. Lett. **89**, 130401 (2002).
[33] T. Lahaye, C. Menotti, L. Santos, M. Lewenstein, and T. Pfau, Rep. Prog. Phys. **72**, 126401 (2009).
[34] A. Griesmaier, J. Stuhler, T. Koch, M. Fattori, T. Pfau, and S. Giovanazzi, Phys. Rev. Lett. **97**, 250402 (2006).
[35] Y. Tang, A. Sykes, N. Q. Burdick, J. L. Bohn, and B. L. Lev, Phys. Rev. A **92**, 022703 (2015).
[36] H. Jing, Phys. Lett. A **306**, 91 (2002).